Decentralized Energy Management of Power- and Hydrogen-based Microgrids in Wholesale Electricity Market as Price-maker

Amin Mansour Saatloo, Abbas Mehrabi, *Member*, *IEEE*, Nauman Aslam, *Member*, *IEEE*, and Mousa Marzband, *Senior Member*, *IEEE*

***Abstract*—The global transition toward net zero emissions has accelerated the integration of distributed generators (DGs), particularly renewable energy sources (RESs), energy storage systems, plug-in electric vehicles (PEVs), and fuel-cell electric vehicles (FEVs). Therefore, we propose a decentralized energy management model tailored to the operational dynamics of a community of independent microgrids (MGs) at the transmission level, integrated with DGs, PEVs, FEVs, and hydrogen-based technologies, forming power- and hydrogen-based microgrids (P&HMGs). Managed by a third-party aggregator, P&HMGs strategically participate in the wholesale electricity market (WEM) by consolidating bids and offers. The WEM operates between generators and suppliers. The participating generators in WEM are connected to the transmission level, including power plants and large-scale RESs. The strategic behavior of P&HMGs is modeled using bi-level programming that unveils the potential of P&HMGs to synergize and participate in WEM as a price-maker. Moreover, to cope with the data privacy of P&HMGs and improve the scalability and security of MGs, a fast alternating direction method of multipliers (ADMM) running on a mobile edge computing (MEC) system is proposed as a decentralized energy management approach. Further, a bidirectional long short-term memory (BiLSTM) network considering robust optimization is presented to control the intermittency of electrical load and RESs. The results obtained from case studies confirm a considerable reduction in operation costs in light of the proposed model.**

***Index Terms*—Microgrid, energy management, electric vehicle, energy storage system, green hydrogen, electricity market, uncertainty.**

Manuscript received: January 24, 2025; revised: May 19, 2025; accepted: July 8, 2025. Date of CrossCheck: July 8, 2025. Date of online publication: October 17, 2025.

This work was supported by the PGR scholarship (RDF studentship) at Northumbria University, in part by the UKRI (No. EP/X039900/1), the European Union's Horizon Europe Research and Innovation Programme under the Marie Sklodowska-Curie (No. 101086218), and the Deanship of Scientific Research (DSR) at King Abdulaziz University, Jaddah, Saudi Arabia (No. IPP: 738-135-2025). The authors, therefore, acknowledge with thanks DSR for technical and financial support.

A. M. Saatloo (corresponding author), A. Mehrabi, and N. Aslam are with the Department of Computer and Information Sciences, Northumbria University, Newcastle upon Tyne, UK (e-mail: a.mansour-saatloo@northumbria.ac.uk; abbas.mehrabidavoodabadi@northumbria.ac.uk; nauman.aslam@northumbria.ac.uk).

M. Marzband is with the Department of Electrical & Computer Engineering and Center of Research Excellence in Renewable Energy and Power Systems, Department of Electrical and Computer Engineering, King Abdulaziz University, Jeddah, Saudi Arabia (e-mail: mmarzband@kau.edu.sa).

DOI: 10.35833/MPCE.2025.000076

NOMENCLATURE

A. Sets

$\mathcal{B}_j$	Set of buses connected to bus j
$\mathcal{D}$	Set of loads indexed by d
$\mathcal{G}$	Set of generators indexed by g
$\mathcal{I}$	Set of microgrids indexed by i
$\mathcal{J}$	Set of electrical buses indexed by j, k
$\mathcal{N}$	Set of plug-in electric vehicles (PEVs) indexed by n
$\mathcal{S}_\mathcal{D}, \mathcal{S}_\mathcal{G}$	Sets of mapping demand and generator into buses
$\mathcal{T}$	Set of time slots indexed by t

B. Superscripts

$+, -$	Indicating the maximum and minimum values of the notation
ar, dp	Indicating the notation is associated with arrival and departure of PEVs
ch, dch	Indicating the notation is associated with charging and discharging modes
CtG	Indicating the notation is associated with coordinator-to-grid
$CtMG$	Indicating the notation is associated with coordinator-to-microgrid
GT, G, d	Indicating the notation is associated with gas turbine, generator, and demand
GtC	Indicating the notation is associated with grid-to-coordinator
HtP	Indicating the notation is associated with hydrogen-to-power
$MGtC$	Indicating the notation is associated with microgrid-to-coordinator
PL, HS, ES	Indicating the notation is associated with parking lot (PL), hydrogen refueling station, and electrical storage (ES) system
PtH	Indicating the notation is associated with power-to-hydrogen
RU, RD	Indicating the notation is associated with ramp-up and ramp-down of generators

C. Parameters

η	Efficiency
Φ^{+}, Φ^{-}	The maximum and minimum power of the charging/discharging of PL (MW)
Π^{HPC}	Hydrogen purchasing cost ($/MWh)
Ψ^{Deg}	Degradation cost of ES system ($/MWh)
B_n	Battery capacity (MW)
BD	Bid price of demand in energy ($/MWh)
I	Capacity of PL
L^{EL}, L^{HL}	Electrical and hydrogen loads of microgrids
MC	The marginal cost of generator in energy ($/MWh)
$P^{+,hyd,HS}$	The maximum capacity of hydrogen vector coupling storage (HVCS) in dispensing hydrogen (MW)
P_g^{ini}	Initial output of generator (MW)
$\tilde{p}_{i,t}^{MGtC}$, $\tilde{p}_{i,t}^{CtMG}$	Fixed values of exported power from microgrid to coordinator and from coordinator to microgrid (MW)
P^{W}, P^{PV}	Wind and photovoltaic power (MW)
S	The maximum capacity of transmission line (MW)
RU, RD	Ramp-up and ramp-down limits (MW)
S^{ar}, S^{dp}	Numbers of arriving and departing PEVs
SC^{+}, SC^{-}	The maximum and minimum values of state of charge of PL

D. Binary Decision Variables

ψ	PEV arriving/departing status
ζ	Charging/discharging status of PL and ES system

E. Continuous Decision Variables

$\mathcal{W}^{ch}$, $\mathcal{W}^{dch}$	Numbers of ES charging and discharging switches
Π	Market clearing price ($/MWh)
σ	Dual variable associated with lower-level market clearing problem
θ	Voltage angle (rad)
C^{GT}	Fuel cost of gas turbines ($)
o^{buy}, o^{sell}	Bid and offer prices of coordinator to energy market ($/MWh)
p	Continuous variable used to indicate amount of power associated with charging/discharging of PL and ES system, power-to-hydrogen/hydrogen-to-power of hydrogen refueling station, coordinator-to-microgrid/microgrid-to-coordinator, and gas turbine
e	State of charge of PEVs
$p^{hyd,buy}$	Purchased hydrogen from hydrogen provider company (MW)
$p^{hyd,HS}$	Amount of discharged hydrogen from HS (MW)
sc	State of charge of single PEV

I. Introduction

THE global effort to achieve the net zero target has intensified to integrate plug-in electric vehicles (PEVs) and fuel-cell electric vehicles (FEVs) in order to establish a carbon-free transportation network [1]. In particular, the commitment of the UK to achieve net-zero emissions has translated into a 4-fold increase in the sale of PEVs in recent years [2] with expectations of a substantial 23-fold increase by 2035 [3]. Simultaneously, the contemporary pursuit of clean energy sources has promoted the integration of renewable energy sources (RESs) into power systems. For instance, in line with the target of the UK for a net-zero power system by 2035, the electricity generation in Great Britain (GB) needs to triple. Consequently, to meet this ambitious objective and accommodate a projected 50% surge in electricity demand, the capacities of wind, photovoltaic (PV), and electrical storage (ES) are anticipated to increase by factors of 6, 5, and 10, respectively [3]. However, the integration of numerous intermittent source-load technologies poses operational challenges within power systems. To address these challenges, integrating small-scale technologies into microgrids (MGs) emerges as a promising solution, offering greater operational certainty.

MGs also serve as holistic energy infrastructures, accommodating hydrogen-based technologies such as electrolyzers, hydrogen storage, fuel cells, and FEVs. Countries like the UK have already adopted hydrogen-powered fleets encompassing cars, trucks, buses, and marine vessels. The total demand for hydrogen in the UK is expected to increase by about 20%-35% (250-460 TWh) by 2050 [4]. However, the current predominant method of hydrogen production involves natural gas, contributing to carbon emissions. Integrating hydrogen-based technologies with MGs offers a solution by enabling the production of green hydrogen from RESs. An exemplar is the Orkney Island project in Scotland, showcasing how power system challenges can be addressed by generating hydrogen from RESs [4]. Consequently, the incorporation of green hydrogen as a sustainable energy carrier within MGs unleashes the potential for a carbon-neutral fuel for diverse applications across power- and hydrogen-based MGs (P&HMGs).

Despite the advantages of P&HMGs, various techno-economic challenges have surfaced. One significant challenge pertains to the participation of P&HMGs in wholesale electricity markets (WEMs), which are operated by independent system operators (ISOs) like the National Grid ESO in the UK [5] at the transmission level. Limitations within the WEM may restrict a single P&HMG from bid/offer, and the capacity of an individual P&HMG might not be substantial enough for strategic involvement. However, the collaborative efforts of a community of P&HMGs could potentially overcome these limitations. Inspired by this discussion, the primary objective of this study is to present a new decentralized energy management model for P&HMGs, fostering collaboration and enabling strategic participation as a price-maker in the WEM.

Plenty of research endeavors have been dedicated to evaluating the integration of electric vehicles and MGs with power systems. For instance, in [6], a risk-averse transactive energy scheme was presented for multi-MGs powered exclusively by RESs and integrated with power and gas networks,

where the conditional value-at-risk (CVaR) was applied to manage the risk. In [7], a decentralized real-time charging scheduling and trajectory planning scheme was proposed for on-route PEVs based on the user preferences, in which a greedy-based algorithm was developed to solve the optimization problem. In [8], a blockchain-based vehicle-to-vehicle power trading scheme was introduced, which used the internet connection of vehicle platform enabled by 5G technology, and a game theory was proposed to design a pricing and matching mechanism for vehicles. In [9], an energy management model was introduced for multi-MGs integrated with RESs, which incorporated time-series prediction based on the Gaussian process regression method and an operation model based on model predictive control (MPC). In a similar context, a distributed pricing mechanism was proposed in [10] for multi-MGs to enhance their economic and environmental revenues based on a Nash bargaining game with the objective of maximizing the overall profit, in which electricity and carbon prices were updated based on supply-demand ration. In [11], a deep reinforcement learning based energy management approach was proposed for real-time energy management of MGs, in which the training process was accelerated by proposing a haring-based parallel technique. Moreover, a risk-averse stochastic framework for energy sharing among multi-MGs in medium-level power systems was presented in [12], in which the alternating direction method of multipliers (ADMM) was utilized for market-clearing.

With the growing integration of hydrogen with power systems, numerous studies focused on the optimal operation of power- and hydrogen-based energy systems. In this regard, a robust decentralized local energy market (LEM) clearing model built upon a fast ADMM for a community of P&HMGs was proposed in [13], where power was transmitted via power lines and hydrogen was transferred via trucks. In a similar context, an ADMM-based peer-to-peer model for power and hydrogen trading among integrated power and transportation systems was proposed in [14], which considered delivery and payment time, physical location, and communication. In [15], a mobile power and hydrogen storage system was proposed for the distribution level to transport power and hydrogen from high penetrated points to high demand points. In addition, a fuzzy information gap decision theory (IGDT) was used to model the uncertainty of RESs. In [16], a deep reinforcement learning based energy management strategy was developed for plug-in FEVs to improve the balance of fuel cost and battery degradation and maintenance, where the trade between different objectives was obtained using a multi-objective optimization. In [17], a day-ahead scheduling paradigm was proposed for PEVs and FEVs in a local multi-energy system, in which an incentive-based response program was presented to improve the flexibility of the energy system. Furthermore, a multi-objective IGDT/robust approach was taken into account to handle the uncertainty. In [18], a two-stage scheduling model was proposed for optimal operation of hydrogen storage integrated with RESs and power to hydrogen and heat, where the first stage optimized day-ahead economic while the second stage dealt with intra-day decisions. In addition, a decentralized ADMM-based policy was presented in [19] for adjusting hydrogen refueling service fees at hydrogen refueling stations (HRSs) to minimize the operation cost, travel cost, and environmental cost of integrated power and transportation networks.

However, P&HMGs have been considered as price-takers in the above-reviewed studies. Shifting toward price-maker behavior, a stochastic bi-level model was presented in [20] for active distribution networks with high penetration of distributed generators in WEM as price-maker. In [21], the impact of integrated demand response was evaluated on the price-maker behavior of a large multi-energy consumer. In [22], a robust bi-level scheme was proposed for multi-energy service providers as price-maker in integrated power and natural gas markets. In [23], a bi-level model was introduced for interaction of PEVs and PEV aggregators for the purpose of frequency regulation, in which the upper level maximized the profit of aggregators and the lower level minimized the cost of PEVs.

Concerning uncertainty management, different approaches have been proposed. For example, a two-stage adaptive robust optimization (RO) was carried out in [24] for controlling the uncertainty of PEV stations. In [25], a hybrid adaptive stochastic-robust method with a solution based on affine policy was established for P&HMGs, in which the final problem was recast as a mixed-integer linear programming (MILP) to minimize the expected cost. In [26], an energy management model was proposed for wind power producer and electric vehicle charging considering an information entropy theory to control wind producer uncertainty in day-ahead electricity market. In this study, Stackelberg game was employed to model the transactions between electric vehicles and wind producer, in which transactions were based on blockchain technology. In [27], a hybrid robust/stochastic uncertainty model was presented for optimal operation of a hybrid power, heat, and hydrogen energy system, in which the RO handled the uncertainty associated with day-ahead decisions and the stochastic model dealt with the uncertainties concerning intra-day and real-time decisions.

With the growing integration of small-scale power and hydrogen technologies into MGs, there exists a substantial need to establish an infrastructure for the optimal operation of P&HMGs. Although plenty of studies focused on the operation of MGs, there are still a series of research gaps (RGs) as listed below.

1) RG1: the focus of many previous studies, for example [9]-[11] and [13], was on MGs as price-takers. However, a community of multiple MGs subject to preserving their privacy can work together to strategically participate in the WEM as a price-maker.

2) RG2: in order to advance P&HMGs and enable their strategic participation in the WEM, there is a critical requirement for privacy-preserving models that unite P&HMGs as a price-maker, allowing them to bid/offer in the WEM. Previously proposed price-maker models [20]-[22] have a centralized framework, which renders them inefficient for multi-agent communities.

3) RG3: previous studies [24]-[26] mainly focused on classic uncertainty management models. However, the development of a hybrid learning-robust-based method for handling uncertain parameters in P&HMGs is vital for informed strategic decision-making.

To bridge these gaps, the following innovations are presented in this paper.

1) A decentralized energy management model for a community of independent P&HMGs is presented. This model empowers P&HMGs to integrate PEVs and FEVs and strategically participate in the WEM. The strategic bid/offer in the WEM enables the P&HMGs to manipulate the WEM for their benefit. The proposed model is structured as a bi-level optimization, in which the P&HMGs are modeled at the upper level while the power system is modeled at the lower level. This addresses RG1.

2) A decentralized energy management approach based on fast ADMM, accelerated by the Nesterov acceleration method, is proposed. Additionally, the mobile edge computing (MEC) system is proposed for the communication of P&HMGs. In light of this proposal, P&HMGs are able to solve their problem on an isolated edge server at their premise, resulting in preserved data privacy, enhanced security and scalability, and reduced complexity. This addresses RG2.

3) A hybrid bidirectional long short-term memory (BiLSTM) network considering robust optimization is developed to manage the uncertainty. The BiLSTM is chosen to overcome the limitations of the long short-term memory (LSTM), particularly its tendency to overlook future data features. Moreover, it demonstrates high efficacy in predicting time series data owing to its bidirectional memory unit, which enables it to capture information from both past and future features. The BiLSTM network is trained to learn the electrical load pattern of P&HMGs and is used to forecast the load for the next day. However, since the RES output depends on forecasts, which are usually provided by an external company like the Met office in the UK, and the related profiles are still uncertain, an RO is put forward. This addresses RG3.

4) A new mathematical formulation for P&HMGs as a price-maker to achieve the optimal solution is presented. To do so, the bi-level optimization problem is transformed into a single-level mathematical program with equilibrium constraints (MPEC) by deriving Karush-Kuhn-Tucker (KKT) conditions and applying the strong duality theory. Then, after implementing the proposed approach based on the fast ADMM and MEC system, the decentralized problem is reformulated as a mixed-integer convex quadratic programming (MICQP) so that the optimal solution can be found.

II. Framework of P&HMGs

The considered framework encompasses IEEE 6-bus system including four generators (G1-G4) and two loads, and a community of independent P&HMGs connected to bus 5, as depicted in Fig. 1. Each P&HMG constitutes wind turbines (WTs) and PV panels, a parking lot (PL) for PEVs, an ES system, gas turbines (GTs), hydrogen vector coupling storage (HVCS), HRS, fuel cells, and electrical load. The HVCS serves to interlink power and hydrogen vectors by converting power solely from RESs into hydrogen gas for storage. The produced hydrogen can be utilized to supply FEVs or converted back into power through fuel cells. Furthermore, in instances of hydrogen scarcity, the P&HMG operator can procure hydrogen from a dedicated hydrogen company (HC). Coordination of the P&HMGs is overseen by a third-party entity, i. e., coordinator, which aggregates bids/offers from the P&HMGs and represents them in the WEM. The participation of the coordinator in the WEM is strategic, which means it can manipulate the WEM prices for the benefit of P&HMGs. The strategic interaction is modeled as bi-level programming, with the community of P&HMGs serving as the leader at the upper level and the power system acting as the follower at the lower level.

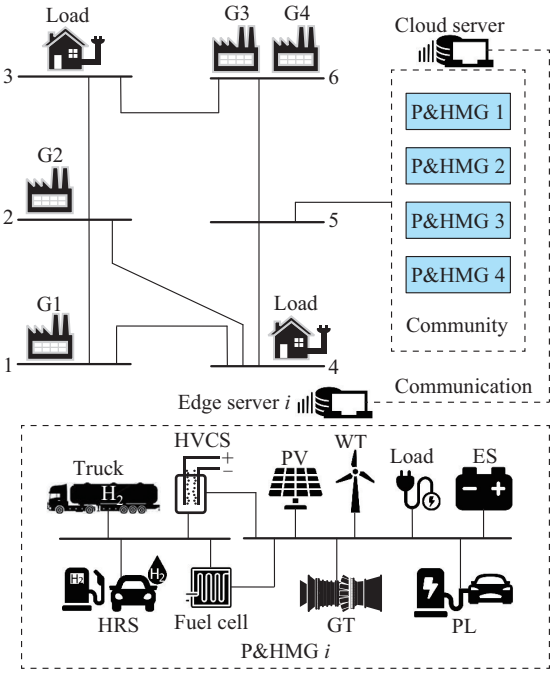

Fig. 1. Considered framework encompassing IEEE 6-bus system and a community of independent P&HMGs.

The coordinator submits a bid/offer (both in terms of power quantity and price) to the lower level, where the WEM is cleared. Subsequently, upon WEM clearance based on the upper-level submission, the resulting cleared price is relayed back to the upper level for the scheduling of P&HMGs. In other words, the power quantity and price submitted by the coordinator to the WEM are external variables at the lower level, while the market clearing price, derived from WEM clearance at the lower level, is an external variable at the upper level.

III. Problem Formulation

This section presents the mathematical formulation of the proposed model. In general, the model comprises two levels: P&HMGs are modeled at the upper level (Section III-A), while the power system is modeled at the lower level (Section III-B). The objective of the upper level is to minimize the operaton cost of the P&HMGs, whereas the objective of

the lower level is to maximize the social welfare.

All the assets of the P&HMGs, including PLs, HRSs, and ES systems, are modeled at the upper level. The upper level also incorporates power and hydrogen balance constraints for the P&HMGs, as well as the RO for managing uncertainties in RESs. Similarly, all the assets of the power system and their associated energy balance constraints are modeled at the lower level. Section III-C then derives the KKT conditions for the lower-level problem. By doing so, the lower-level problem can be replaced with a set of constraints and integrated with the upper-level problem. However, the resulting single-level problem is still nonlinear. Section III-D tackles the non-linearity issue by enforcing strong duality theory. After that, Section III-E introduces the proposed decentralized energy management approach, which splits the problem into sub-problems based on the number of agents involved. Finally, Section III-G describes the BiLSTM network which is used to forecast the load.

A. Upper Level: Minimizing Operation Cost of P&HMGs

At the upper level of the problem, P&HMGs are modeled. The objective of the community is to minimize the total cost f^U as stated in (1), which includes four terms. The first term is the operation cost of GTs, the second term is the degradation cost of ES systems, the third term is the cost of purchasing hydrogen from HC, and the last term is the cost of traded power in the WEM. In this objective function, the decision variable Π_t is the WEM price and belongs to the lower level.

$$\min f^U = \sum_{t\in\mathcal{T}}\Bigg\{\sum_{i\in\mathcal{I}}\Bigg[C_{i,t}^{GT}+\Psi^{Deg}\left(\eta^{ch,ES}p_{i,t}^{ch,ES}+\frac{p_{i,t}^{dch,ES}}{\eta^{dch,ES}}\right)+\Pi^{HPC}p_{i,t}^{hyd,buy}\Bigg]+\Pi_t(p_t^{GtM}-p_t^{MtG})\Bigg\} \tag{1}$$

1) PL

The PL model is defined by (2a)-(2n). At each time slot, the number of arriving and departing PEVs is computed by (2a) and (2b), respectively. The total number of PEVs in a PL is determined by (2c), ensuring that it does not exceed the maximum capacity specified in (2d). Similarly, the power capacity of a PL at each time slot is determined by the arriving PEV capacities (2e) and departing PEV capacities (2f), constrained by (2g). Moreover, the charging and discharging power of a PL is bounded within secure ranges, as defined by (2h) and (2i), respectively. Further, (2j) is introduced to prevent simultaneous charging and discharging modes. Lastly, the state of charge (SoC) of a PL can be determined based on the SoC of arriving PEVs (2k) and departing PEVs (2l) using (2m), which is limited by (2n).

$$I_{i,t}^{ar}=\sum_{n\in\mathcal{N}}\psi_{n,i,t}^{ar} \tag{2a}$$

$$I_{i,t}^{dp}=\sum_{n\in\mathcal{N}}\psi_{n,i,t}^{dp} \tag{2b}$$

$$I_{i,t}=I_{i,t-1}+I_{i,t}^{arv}-I_{i,t}^{dp} \tag{2c}$$

$$I_{i,t}\le I_i^{+} \tag{2d}$$

$$S_{i,t}^{ar}=\sum_{n\in\mathcal{N}}B_n\psi_{n,i,t}^{ar} \tag{2e}$$

$$S_{i,t}^{dp}=\sum_{n\in\mathcal{N}}B_n\psi_{n,i,t}^{dp} \tag{2f}$$

$$S_{i,t}=S_{i,t-1}+S_{i,t}^{ar}-S_{i,t}^{dp} \tag{2g}$$

$$I_{i,t}\zeta_{i,t}^{ch}\Phi_i^{ch,-}\le p_{i,t}^{ch,PL}\le I_{i,t}\zeta_{i,t}^{ch}\Phi_i^{ch,+} \tag{2h}$$

$$I_{i,t}\zeta_{i,t}^{dch}\Phi_i^{dch,-}\le p_{i,t}^{dch,PL}\le I_{i,t}\zeta_{i,t}^{dch}\Phi_i^{dch,+} \tag{2i}$$

$$\sigma_{i,t}^{ch}+\sigma_{i,t}^{dch}\le 1 \tag{2j}$$

$$e_{i,t}^{ar,PL}=\sum_{n\in\mathcal{N}}B_n\cdot sc_{n,i,t}^{ar}\cdot\psi_{n,i,t}^{ar} \tag{2k}$$

$$e_{i,t}^{dp,PL}=\sum_{n\in\mathcal{N}}B_n\cdot sc_{n,i,t}^{dp}\cdot\psi_{n,i,t}^{dp} \tag{2l}$$

$$e_{i,t}^{PL}=e_{i,t-1}^{PL}+e_{i,t-1}^{ar,PL}-e_{i,t-1}^{dp,PL}+\eta_i^{ch,PL}p_{i,t}^{ch,PL}-\frac{p_{i,t}^{dch,PL}}{\eta_i^{dch,PL}} \tag{2m}$$

$$SC_i^{-}\cdot S_{i,t}\le e_{i,t}^{PL}\le SC_i^{+}\cdot S_{i,t} \tag{2n}$$

2) HRS

The considered HRS is equipped with an HVCS to couple hydrogen and power from RESs. Equation (3a) indicates the SoC of the HVCS, which is limited by (3b). The power-to-hydrogen (PtH) conversion rate is limited to the RES output power, as specified by (3c). In addition, (3e) accounts for the physical constraint of the HVCS in dispensing hydrogen. Similarly, the physical limitation of the fuel cells in the hydrogen-to-power (HtP) conversion is considered via (3f).

$$e_{i,t}^{HS}=e_{i,t-1}^{HS}+\eta_i^{PtH}p_{i,t}^{PtH}-p_{i,t}^{hyd,HS} \tag{3a}$$

$$e_i^{-,HS}\le e_{i,t}^{HS}\le e_i^{+,HS} \tag{3b}$$

$$p_{i,t}^{PtH}\le P_{i,t}^{W}+P_{i,t}^{PV} \tag{3c}$$

$$P_i^{-,PtH}\le p_{i,t}^{PtH}\le P_i^{+,PtH} \tag{3d}$$

$$p_{i,t}^{hyd,HS}\le P_i^{+,hyd,HS} \tag{3e}$$

$$P_i^{-,HtP}\le p_{i,t}^{HtP}\le P_i^{+,HtP} \tag{3f}$$

3) ES Systems

Equation (4a) delineates the SoC of the ES system, subject to the constraint imposed by (4b). Equations (4c) and (4d) serve to impose restrictions on the charging and discharging rates, respectively. Additionally, (4e) ensures that the ES system is not engaged in simultaneous charging and discharging modes, while (4f) guarantees that the SoC of the ES system remains unchanged from its initial value at the beginning of the day to its final state at the end of the day. Further, (4g) and (4h) are considered to count the number of switches to charging and discharging points, respectively. The total number of allowed switches according to life cycle is limited by (4i). Equations (4j)-(4l) are linearized forms of (4g) and the same relations can be applied for the linearization of (4h).

$$e_{i,t}^{ES}=e_{i,t-1}^{ES}+\eta_i^{c,ES}p_{i,t}^{ch,ES}-\frac{p_{i,t}^{dch,ES}}{\eta_i^{dch,ES}} \tag{4a}$$

$$e_i^{-,ES}\le e_{i,t}^{ES}\le e_i^{+,ES} \tag{4b}$$

$$P_i^{ch,-,ES}\zeta_{i,t}^{ch,ES}\le p_{i,t}^{ch,ES}\le P_i^{ch,+,ES}\zeta_{i,t}^{ch,ES} \tag{4c}$$

$$P_i^{dch,-,ES}\zeta_{i,t}^{dch,ES} \le p_{i,t}^{dch,ES} \le P_i^{dch,+,ES}\zeta_{i,t}^{dch,ES} \quad (4d)$$

$$\zeta_{i,t}^{ch,ES} + \zeta_{i,t}^{dch,ES} \le 1 \quad (4e)$$

$$e_{i,t=0}^{D,ES} = e_{i,t=24}^{D,ES} \quad (4f)$$

$$\mathcal{W}_{i,t}^{ch} = \zeta_{i,t}^{ch,ES} - \zeta_{i,t}^{ch,ES}\zeta_{i,t-1}^{ch,ES} \quad (4g)$$

$$\mathcal{W}_{i,t}^{dch} = \zeta_{i,t}^{dch,ES} - \zeta_{i,t}^{dch,ES}\zeta_{i,t-1}^{dch,ES} \quad (4h)$$

$$\sum_{t\in\mathcal{T}}(\mathcal{W}_{i,t}^{ch} + \mathcal{W}_{i,t}^{dch}) \le \mathcal{W}_i^{+} \quad (4i)$$

$$\mathcal{W}_{i,t}^{ch} \le \zeta_{i,t}^{ch,ES} \quad (4j)$$

$$\mathcal{W}_{i,t}^{ch} \le 1 - \zeta_{i,t-1}^{ch,ES} \quad (4k)$$

$$\mathcal{W}_{i,t}^{ch} \ge \zeta_{i,t}^{ch,ES} - \zeta_{i,t-1}^{ch,ES} \quad (4l)$$

4) Power and Hydrogen Balance Constraints

Equation (5a) defines the power balance constraint applicable to each P&HMG. Equation (5b) represents the coupling constraint between P&HMGs and the coordinator, ensuring that the power supplied from the coordinator to a P&HMG matches the received amount. Equation (5c) imposes the power balance constraint between the coordinator and the upstream grid. Finally, (5d) governs the hydrogen balance within each P&HMG.

$$P_{i,t}^{W} + P_{i,t}^{PV} - p_{i,t}^{MGtC} + p_{i,t}^{GT} + p_{i,t}^{dch,ES} + p_{i,t}^{HtP} + p_{i,t}^{dch,PL} - p_{i,t}^{ch,ES} - p_{i,t}^{PtH} - p_{i,t}^{ch,PL} - L_{i,t}^{el} = 0 \quad (5a)$$

$$p_{i,t}^{CtMG} + p_{i,t}^{MGtC} = 0 \quad (\gamma_{i,t}) \quad (5b)$$

$$\sum_{i\in\mathcal{I}} p_{i,t}^{CtMG} = p_t^{GtC} - p_t^{CtG} \quad (5c)$$

$$p_{i,t}^{hyd,buy} + p_{i,t}^{hyd,HS} - \frac{p_{i,t}^{HtP}}{\eta^{HtP}} - L_{i,t}^{HL} = 0 \quad (5d)$$

5) RO

In this study, an RO based on an uncertainty budget set is applied to control the uncertainty of RESs [28]. The RO does not require much information about the uncertain parameters and is free from any probability distribution function, which makes it superior to stochastic approaches. In the RO, the uncertainty budget $\Gamma_{i,t}$ varies from 0 (implying no uncertainty) to 2, which is the number of RESs and implies consideration of full uncertainty. By increasing the uncertainty budget value, the robustness of the optimization increases, which makes the solution more conservative. This means that for higher values of $\Gamma_{i,t}$, the RO dispatches less RESs that cause higher operation cost. However, the resulting cost for a given value of $\Gamma_{i,t}$ is the minimum achievable under the worst-case uncertainty realization. For instance, for $\Gamma_{i,t}=2$, the RO will consider the maximum deviation of the RES (wind and PV) output. However, for a value less than 2, the RO will find the worst-case scenario to split the deviation between wind and PV. For instance, for $\Gamma_{i,t}=1$, the RO may consider 0.25 (25%) of the maximum deviation for PV and 0.75 (75%) of the maximum deviation for wind as the worst-case scenario. Equations (6a)-(6c) define the robust counterpart of the problem and, in the RO, these relations are taken into account instead of (5a). In these relations, $\alpha_{i,t}$ and $\beta_{i,t}$ are the dual variables and ϕ denotes the other terms in (5a). Further mathematical details of the RO can be found in [13].

$$P_{i,t}^{W} + P_{i,t}^{PV} - \alpha_{i,t}^{W} - \alpha_{i,t}^{PV} - \beta_{i,t}\Gamma_{i,t} + \phi \ge 0 \quad (6a)$$

$$\beta_{i,t} + \alpha_{i,t}^{W} \ge P_{i,t}^{W} \quad (6b)$$

$$\beta_{i,t} + \alpha_{i,t}^{PV} \ge P_{i,t}^{PV} \quad (6c)$$

B. Lower Level: Maximizing Social Welfare

The lower-level problem clears the WEM by maximizing social welfare f^L in (7a). Equation (7b) represents the power balance of the entire power system. The associated dual variable $\Pi_{j,t}$ of this equation determines the WEM price, which is sent to the upper level. Equation (7c) enforces the maximum output power limit of generators, while (7d) and (7e) handle the ramp-up limitations. Similarly, (7f) and (7g) address the ramp-down limitations. Equation (7h) restricts the consumption level of retailers. Additionally, security constraints for transmission lines are represented through (7i)-(7k), where (7i) ensures that the power flow does not exceed the capacity of the line, (7j) maintains the secure bus angles, and (7k) determines the reference bus in the power system.

$$\max f^L = \sum_{t\in\mathcal{T}}\left(\sum_{d\in\mathcal{D}} BD_{d,t}\cdot p_{d,t} - o_t^{sell}p_t^{MtG} + o_t^{buy}p_t^{GtM} - \sum_{g\in\mathcal{G}} MC_g\cdot p_{g,t}\right) \quad (7a)$$

$$\sum_{d:(d,j)\in\mathcal{S}_{\mathcal{D}},d=1} p_{d,t} - (p_t^{MtG} - p_t^{GtM}) - \sum_{g:(g,j)\in\mathcal{S}_{\mathcal{G}},g=1} p_{g,t} = \sum_{k\in\mathcal{B}_j,j=1} B_{j,k}(\theta_{j,t}-\theta_{k,t}) \quad \forall j,\forall t \quad (\Pi_{j,t}) \quad (7b)$$

$$0 \le p_{g,t} \le P_g^{+} \quad \forall g,\forall t \quad (\sigma_{g,t}^{-},\sigma_{g,t}^{+}) \quad (7c)$$

$$p_{g,t} - P_g^{ini} \le RU_g \quad \forall g,\forall t=1 \quad (\sigma_{g,t}^{RU}) \quad (7d)$$

$$p_{g,t} - p_{g,t-1} \le RU_g \quad \forall g,\forall t>1 \quad (\sigma_{g,t}^{RU}) \quad (7e)$$

$$P_g^{ini} - p_{g,t} \le RD_g \quad \forall g,\forall t=1 \quad (\sigma_{g,t}^{RD}) \quad (7f)$$

$$p_{g,t-1} - p_{g,t} \le RD_g \quad \forall g,\forall t>1 \quad (\sigma_{g,t}^{RD}) \quad (7g)$$

$$0 \le p_{d,t} \le P_{d,t}^{+} \quad \forall d,\forall t \quad (\sigma_{d,t}^{-},\sigma_{d,t}^{+}) \quad (7h)$$

$$B_{j,k}(\theta_{j,t}-\theta_{k,t}) \le S_{j,k}^{+} \quad \forall j,\forall k\in\mathcal{B}_j,\forall t \quad (\sigma_{j,k,t}^{S}) \quad (7i)$$

$$\theta^{-} \le \theta_{j,t} \le \theta^{+} \quad \forall j,\forall t \quad (\sigma_{j,t}^{\theta,-},\sigma_{j,t}^{\theta,+}) \quad (7j)$$

$$\theta_{j,t} = 0 \quad \forall j=1,\forall t \quad (\sigma_{j,t}^{\theta}) \quad (7k)$$

C. KKT Conditions of Lower-level Problem

In order to reformulate the presented intractable bi-level optimization problem into a tractable single-level MPEC, the KKT conditions of the lower-level problem, i.e., (7a)-(7k), are derived as (8a)-(8q). The single-level MPEC comprises the upper-level problem, i.e., (1)-(5d), constraints of the lower-level problem, i.e., (7b)-(7k), and (8a)-(8q).

$$-BD_{d,t} + \Pi_{j:(j,d)\in\mathcal{S}_{\mathcal{D}},t} + \sigma_{d,t}^{+} - \sigma_{d,t}^{-} - \sigma_{d,t}^{d,-} = 0 \quad \forall d,\forall t \quad (8a)$$

$$o_t^{sell} - \Pi_{j,t} = 0 \quad \forall t \quad (8b)$$

$$-o_t^{buy} + \Pi_{j,t} = 0 \quad \forall t \quad (8c)$$

$$MC_g - \Pi_{j:(j,g)\in\mathcal{S}_{\mathcal{G}},t} + \sigma_{g,t}^{+} - \sigma_{g,t}^{-} + \sigma_{g,t}^{RU} - \sigma_{g,t+1}^{RU} - \sigma_{g,t}^{RD} + \sigma_{g,t+1}^{RD} = 0 \quad \forall g,\forall t<24 \quad (8d)$$

$$MC_g - \Pi_{j:(j,g)\in\mathcal{S}_g,t} + \sigma^{+}_{g,t} - \sigma^{-}_{g,t} + \sigma^{RU}_{g,t} - \sigma^{RD}_{g,t} = 0 \quad \forall g, \forall t = 24 \tag{8e}$$

$$\sum_{k\in\mathcal{B}_j, j=1} [B_{j,k}(\Pi_{j,t} - \Pi_{k,t}) + B_{j,k}(\sigma^{S}_{j,k,t} - \sigma^{S}_{k,j,t}) + \sigma^{\theta,+}_{j,t} - \sigma^{\theta,-}_{j,t} + \sigma^{\theta}_{j=1,t} = 0 \quad \forall j, \forall t \tag{8f}$$

$$0 \le p_{g,t} \perp \sigma_{g,t} \ge 0 \quad \forall g, \forall t \tag{8g}$$

$$0 \le (P^{+}_{g} - p_{g,t}) \perp \sigma^{+}_{g,t} \ge 0 \quad \forall g, \forall t \tag{8h}$$

$$0 \le p_{d,t} \perp \sigma^{-}_{d,t} \ge 0 \quad \forall g, \forall t \tag{8i}$$

$$0 \le (P^{+}_{d,t} - p_{d,t}) \perp \sigma^{+}_{d,t} \ge 0 \quad \forall g, \forall t \tag{8j}$$

$$0 \le (RU_g - p_{g,t} + P^{ini}_{g}) \perp \sigma^{RU}_{g,t} \ge 0 \quad \forall g, \forall t \tag{8k}$$

$$0 \le (RU_g - p_{g,t} + p_{g,t-1}) \perp \sigma^{RU}_{g,t} \ge 0 \quad \forall g, \forall t \tag{8l}$$

$$0 \le (RD_g - P^{ini}_{g} + p_{g,t}) \perp \sigma^{RD}_{g,t} \ge 0 \quad \forall g, \forall t = 1 \tag{8m}$$

$$0 \le (RD_g - p_{g,t-1} + p_{g,t}) \perp \sigma^{RD}_{g,t} \ge 0 \quad \forall g, \forall t > 1 \tag{8n}$$

$$0 \le [S^{+}_{j,k} - B_{j,k}(\theta_{j,t} - \theta_{k,t})] \perp \sigma^{S}_{j,k,t} \ge 0 \quad \forall j, \forall k \in \mathcal{B}_j, \forall t \tag{8o}$$

$$0 \le (\theta_{j,t} - \theta^{-}) \perp \sigma^{\theta,-}_{j,t} \ge 0 \quad \forall j, \forall t \tag{8p}$$

$$0 \le (\theta^{+} - \theta_{j,t}) \perp \sigma^{\theta,+}_{j,t} \ge 0 \quad \forall j, \forall t \tag{8q}$$

D. Linearization of Single-Level MPEC

The single-level MPEC is still nonlinear due to the product of price and quantity of power $\Pi_t(p^{GtM}_t - p^{MtG}_t)$ in the objective function (1) and the complementary conditions in (8g)-(8r). Regarding the nonlinear term in (1), the following actions are put forward. Firstly, the strong duality condition is enforced as (9a). After that, by substituting o^{buy}_t, o^{sell}_t with $\Pi_{j,t}$ according to the relations (8b) and (8c), the linear equivalent of $\Pi_t(p^{GtM}_t - p^{MtG}_t)$ is Ψ_t, as stated in (9b).

Moreover, all constraints expressed in the form of $0 \le f \perp g \ge 0$ can be restated in the linear form of $f \ge 0$, $g \ge 0$, $f \le yM$, and $g \le (1-y)M$ using the Big-M method [29], where y and M are a binary auxiliary variable and a big number, respectively.

$$\sum_{t\in\mathcal{T}}\left(\sum_{d\in\mathcal{D}} BD_{d,t}\cdot p_{d,t} - o^{sell}_t p^{MtG}_t + o^{buy}_t p^{GtM}_t - \sum_{g\in\mathcal{G}} MC_g \cdot p_{g,t}\right) = \sum_{d\in\mathcal{D}} \sigma^{+}_{d,t} P^{+}_{d,t} + \sum_{g\in\mathcal{G}} (\sigma^{+}_{g,t} P^{+}_{g} + \sigma^{RU}_{g,t=1} P^{ini}_{g} - \sigma^{RU}_{g,t} \cdot RU_g - \sigma^{RD}_{g,t=1} P^{ini}_{g} - \sigma^{RD}_{g,t} \cdot RD_g) - \sum_{j\in\mathcal{J}} (\sigma^{\theta,-}_{j,t}\theta^{-} - \sigma^{\theta,+}_{j,t}\theta^{+}) + \sum_{j\in\mathcal{J}_k}\sum_{k\in\mathcal{J}_j\neq k} \mu^{S}_{j,k,t} S^{+}_{j,k} \tag{9a}$$

$$o^{buy}_t p^{GtM}_t - o^{sell}_t p^{MtG}_t = \Pi_t(p^{GtM}_t - p^{MtG}_t) = \Psi_t \tag{9b}$$

$$\Psi_t = \sum_{g\in\mathcal{G}} MC_g \cdot p_{g,t} - \sum_{d\in\mathcal{D}} BD_{d,t}\cdot p_{d,t} + \sum_{d\in\mathcal{D}} \sigma^{+}_{d,t} P^{+}_{d,t} + \sum_{g\in\mathcal{G}} (\sigma^{+}_{g,t} P^{+}_{g} + \sigma^{RU}_{g,t=1} P^{ini}_{g} - \sigma^{RU}_{g,t} \cdot RU_g - \sigma^{RD}_{g,t=1} P^{ini}_{g} - \sigma^{RD}_{g,t} \cdot RD_g) - \sum_{j\in\mathcal{J}} (\sigma^{\theta,-}_{j,t}\theta^{-} - \sigma^{\theta,+}_{j,t}\theta^{+}) + \sum_{j\in\mathcal{J}_k}\sum_{k\in\mathcal{J}_j\neq k} \mu^{S}_{j,k,t} S^{+}_{j,k} \tag{9c}$$

E. Decentralized Energy Management Approach

The proposed approach based on the fast ADMM addresses significant challenges inherent in centralized approaches. The ADMM was presented by [30] and then has been widely applied to power system applications. However, the traditional version of the ADMM is not sufficient to handle large-scale problems. Hence, in this study, an accelerated version of the ADMM based on the Nesterov acceleration method is proposed, in which the fast ADMM has a lower convergence rate of $O(1/Z^2)$ in comparison with the traditional ADMM $O(1/Z)$ [31], where Z is the iteration counter. Additionally, the MEC system is presented to build an efficient computation and communication infrastructure. By doing so, each of the P&HMGs is allocated an edge server, in which the edge servers are isolated from the rest of the system. In addition, the coordinator is equipped with a cloud server that communicates with the P&HMGs.

To mathematically decompose the problem utilizing the fast ADMM, the complicating constraint (5b) undergoes relaxation through the formation of an augmented Lagrangian function $\mathcal{L}$, as represented by (10a). In this relation, $\gamma_{i,t}$ is the dual variable corresponding to (5b), and ρ is the penalty factor. After that, since the complicating constraint no longer exists in the problem, it can be easily decomposed. The local problem of the coordinator LP^{C} and each of the P&HMGs LP^{MG}_i are introduced as (10b) and (10c), respectively.

$$\mathcal{L} = f^{U} + \sum_{t\in\mathcal{T}}\left[\gamma_{i,t}(p^{CtMG}_{i,t} + p^{MGtC}_{i,t}) + \frac{\rho}{2}\|p^{CtMG}_{i,t} + p^{MGtC}_{i,t}\|^2_2\right] \tag{10a}$$

$$LP^{C}: \begin{cases} \min\left[\sum_{t\in\mathcal{T}} \Psi_t + \gamma_{i,t}(p^{CtMG}_{i,t} + \tilde{p}^{MGtC}_{i,t}) + \frac{\rho}{2}\|p^{CtMG}_{i,t} + \tilde{p}^{MGtC}_{i,t}\|^2_2\right] \\ \text{s.t. (8a)-(8q)} \end{cases} \tag{10b}$$

$$LP^{MG}_i: \begin{cases} \min \sum_{t\in\mathcal{T}}\left[C^{GT}_{i,t} + \Psi^{Deg}(\eta^{ch,ES} p^{ch,ES}_{i,t} + \eta^{dch,ES} p^{dch,ES}_{i,t}) + \Pi^{HPC}_{i,t} p^{hyd}_{i,t} + \gamma_{i,t}(\tilde{p}^{CtMG}_{i,t} + p^{MGtC}_{i,t}) + \frac{\rho}{2}\|\tilde{p}^{CtMG}_{i,t} + p^{MGtC}_{i,t}\|^2_2\right] \\ \text{s.t. (2b)-(5a), (5d)} \end{cases} \tag{10c}$$

In these problems, the existing second norms $\|\cdot\|^2_2$ present non-linearity. Yet, by reformulating these terms with $(\cdot)^2$, the problem becomes an MICQP whose optimal solution can be obtained. The iterative procedure for solving the problem is delineated in Algorithm 1. Initially, dual variables and exchanged power quantities between the coordinator and P&HMGs are initialized. Following this, in the first iteration, each of the entities, including P&HMGs and the coordinator, solves their local problem on the allocated edge servers and cloud server at their premise, respectively. Subsequently, P&HMGs share the obtained power to be exchanged with the coordinator and then the values of dual variables are transmitted to the edge servers for the next iteration after being updated on the cloud server. The cloud server also updates the acceleration parameter based on the Nesterov acceleration method (line 13) and the accelerated dual variable $\hat{\gamma}_{i,t}$ (line 14) for the subsequent iteration. This iterative process persists until the convergence criteria are satisfied.

Algorithm 1: iterative procedure for solving problem

1. Form augmented Lagrangian function as (10a)
2. Derive objective function of each coordinator and P&HMGs as (10b) and (10c)
3. Initialize $Z, \alpha_t, \rho, er, \gamma_{i,t}, \tilde{p}_{i,t}^{MGtC}, \tilde{p}_{i,t}^{CtMG}$, where er is the acceptable error
4. **while** $\max\{er\} \le \epsilon$ **do**
5. **for** $i \in \mathcal{I}$ do
6. Solve subproblem LP_i^{MG} (edge servers)
7. Declare $p_{i,t}^{MGtC}$
8. **end for**
9. Solve LP^C (cloud server)
10. Declare $p_{i,t}^{CtMG}$ (cloud server)
11. Update dual variables (cloud server)
$$\gamma_{i,t}(Z+1) = \hat{\gamma}_{i,t}(Z) + \rho(p_{i,t}^{CtMG} + p_{i,t}^{MGtC})$$
12. Broadcast dual variables (cloud server)
13. Update acceleration parameter (cloud server)
$$\alpha_t(Z+1) = \frac{1+\sqrt{1+4(\alpha_t(Z))^2}}{2}$$
14. Accelerate dual variables (cloud server)
$$\hat{\gamma}_{i,t}(Z+1) = \gamma_{i,t}(Z) + \frac{\alpha_t(Z)-1}{\alpha_t(Z+1)}(\gamma_{i,t}(Z) - \gamma_{i,t}(Z-1))$$
15. Update errors $\|p_{i,t}^{CtMG} + p_{i,t}^{MGtC}\| \le er$ (cloud server)
16. Update iteration index $Z \leftarrow Z+1$
17. **end while**

F. Discussion on Complexity

The computational complexity of the proposed approach is expressed as $O((|\mathcal{I}|+1)Z\tau/\mathcal{M})$, where $\mathcal{M}$ is the number of the MEC system servers; τ represents the complexity of solving a single subproblem per iteration on a server; and $|\mathcal{I}|+1$ is the total number of decision-making participants (P&HMGs and the coordinator). Since each participant is assumed to have its own server, we have $|\mathcal{I}|+1=\mathcal{M}$. This allows the complexity expression to be simplified to $O(Z\tau)$. It is important to note that τ depends entirely on the solver used. In this study, the CPLEX solver is employed, whose basic computational complexity is $O(m^2 n)$, where m is the number of constraints; and n is the number of variables [32].

Regarding the communication overhead, each iteration involves two rounds of message exchanges between the coordinator and the P&HMGs. In the first round, the P&HMGs solve their local optimization problems and send the resulting P^{MGtC} values to the coordinator. In the second round, the coordinator updates the dual variables and broadcasts them back to the P&HMGs. As a result, a total of 8 messages are exchanged per iteration. Hence, the communication complexity can be expressed as $O(8)$.

In addition, the convergence rate of a decentralized approach is typically evaluated based on its worst-case iteration complexity. For the traditional ADMM, this complexity is $O(1/Z)$ or equivalently $O(1/\epsilon)$. This means that after k iterations, the traditional ADMM achieves an error on the order of $O(1/Z)$ or it needs $O(1/\epsilon)$ iterations to reach a solution with an accuracy of ϵ. On the other hand, the proposed approach improves this rate to $O(1/Z^2)$ or $O(1/\sqrt{\epsilon})$, indicating a more efficient convergence with fewer iterations [31].

G. BiLSTM Network

The BiLSTM network is employed for the purpose of forecasting the daily load of P&HMGs. Structurally, a BiLSTM network comprises two layers: a backward hidden layer and a forward hidden layer, mirroring the configuration of LSTM layers. The backward hidden layer processes information from the beginning to the end, capturing features from past to future, while the forward hidden layer operates in the reverse direction, capturing features from future to past. Consequently, the BiLSTM network adeptly captures dependencies in temporal data from both temporal directions, enhancing its understanding of temporal dependencies. Moreover, the bidirectional memory unit mitigates issues related to error accumulation, thereby bolstering the ability of the BiLSTM network to forecast stochastic profiles. An illustrative architecture of a BiLSTM network along with mathematical modeling is presented in Supplementary Material A.

IV. Simulation and Results

A. Case Study

To assess the efficacy of the proposed model, an extensive dataset comprising electrical load profiles from six countries was gathered for training a BiLSTM network [33]. This dataset spans a duration of three years, from January 1, 2015 to December 31, 2017, with a temporal resolution of 30 min. In this investigation, a sliding window approach was employed, utilizing the preceding 96 samples (equivalent to 48 hours) to forecast the subsequent sample. It is noted that the model is trained once and then the extracted features can be saved for forecasting in the future. Subsequently, the proposed model was evaluated using test scenarios based on the IEEE 6-bus and 24-bus systems. Figure 1 illustrates the modified IEEE 6-bus system, wherein four P&HMGs are interconnected to bus 5 at the transmission level, and geographically closed MGs are connected to the same bus of a power system. Additionally, Fig. 1 provides an overview of each P&HMG, as detailed in Section II. For this particular case study, the electrical load profiles of GB, Northern Ireland (NIR), Ireland (IE), and the Netherlands (NL) were scaled down and designated for use within the P&HMGs. To further scrutinize the performance of the proposed model on a larger scale, assessments were conducted on a modified IEEE 24-bus system integrated with six P&HMGs. In this configuration, the electrical load profiles of Belgium (BE) and Hungary (HU) were incorporated for the remaining two P&HMGs. The BiLSTM network was trained and evaluated using Python, while the proposed model was implemented within the GAMS environment. All computational tasks were executed on a server equipped with 64 GB of RAM and a GPU with 12 GB VRAM. It is also to be noted that the scheduling problem is executed for 24 hours with 1-hour time slots.

B. Modified IEEE 6-bus System

To initiate this case study, a BiLSTM network was trained with the above-mentioned dataset, in which 80% and 20%

data of the dataset are dedicated to training and testing purposes, respectively. The BiLSTM network comprises three main layers, with each LSTM layer containing 256, 128, and 32 hidden units, respectively. Additionally, two dropout layers with a probability of 0.5 are considered to avoid co-adaption of neurons. Moreover, the maximum number of epochs and the learning rate are set to be 50 and 0.0001, respectively. For scheduling purposes, a random day (November 14, 2017) was chosen. Figure 2 depicts the regression plots of the BiLSTM network for each dataset and Table I enumerates the three well-known error criteria, i.e., mean absolute error (MAE), mean absolute percentage error (MAPE), and root mean square error (RMSE), to evaluate the performance of the BiLSTM network.

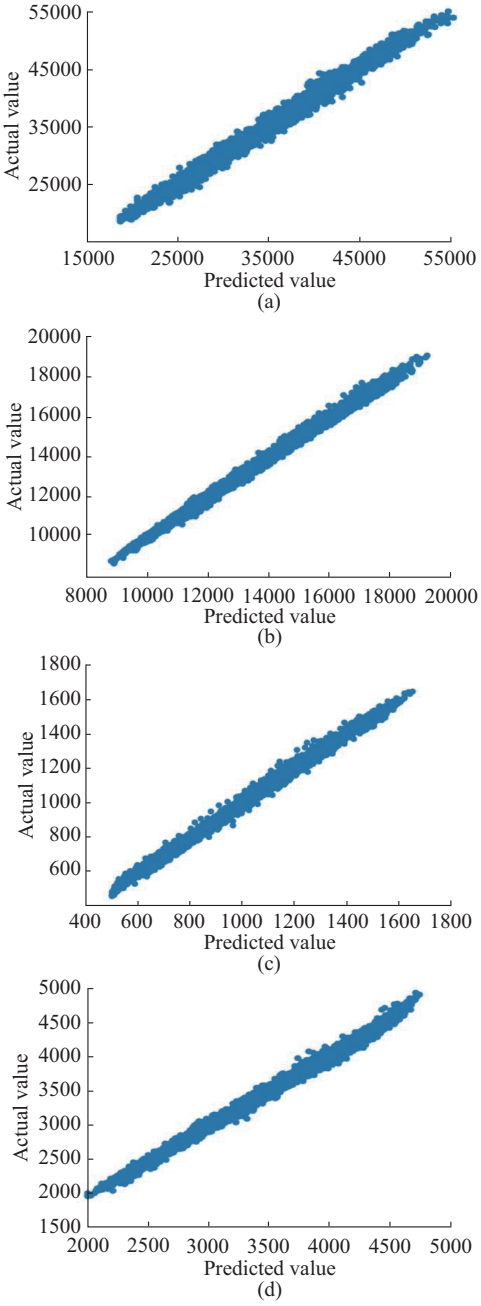

Fig. 2. Regression plots of BiLSTM network for each dataset. (a) GB (P&HMG 1). (b) NL (P&HMG 2). (c) NIR (P&HMG 3). (d) IE (P&HMG 4).

TABLE I
PERFORMANCE ANALYSIS OF BILSTM NETWORK ON NOVEMBER 14, 2017

Dataset	MAE	MAPE	RMSE
GB	380.38	1.29	471.53
NIR	8.89	1.10	11.80
IE	32.53	1.14	47.70
NL	74.03	0.65	86.88

The output forecasted electrical load is supplied to the scheduling problem as an input and the problem is solved based on the proposed approach. Figure 3 demonstrates the commitment of generators and local marginal prices (LMPs). It is evident that the LMPs are correlated with the commitment of generators. During the period from the 1st hour to the 16th hour, the LMPs remain within the range of 12 to 30 $/MWh as G1 and G2 characterized by lower marginal costs, fulfilling the load requirements. However, a notable surge in LMPs occurs between the 17th hour and the 20th hour, attributed to the engagement of high-cost generation units such as G3 and G4, which results in peak LMPs averaging 122.87 $/MWh and reaching 159.22 $/MWh at bus 5. Subsequently, from the 21st hour till the end of the day, LMPs exhibit a decline and stabilize at 12 $/MWh.

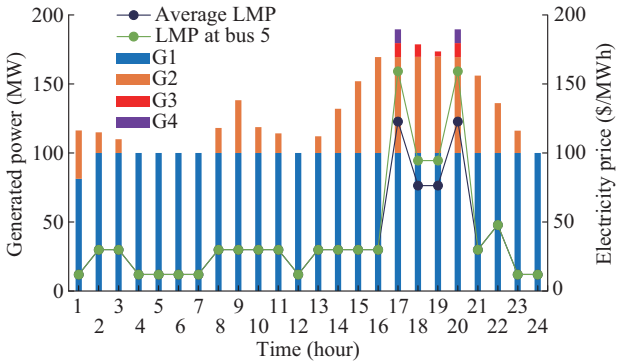

Fig. 3. Commitment of generators and LMPs.

Further, Fig. 4 illustrates the power and hydrogen dispatch of each P&HMG. As can be observed, P&HMGs 1 and 2 utilize their local GTs during the high LMP period, i.e., the 16th hour to the 22nd hour, due to the high operation cost of their GTs. In contrast, P&HMGs 3 and 4 utilize their GTs from the 2nd hour to the 24th hour as they possess low-cost GTs. The charging/discharging behavior of the ES systems follows a similar trend across all P&HMGs. The ES systems are charged during the low LMP period and discharged during peak periods, i.e., the 17th hour to the 20th hour. In addition, the charging pattern of the PLs primarily depends on the arrival and departure times of the PEVs. However, the PLs are mainly discharged between the 17th hour and the 20th hour when the market hits peak LMPs. Moreover, it is perceived that the power has been converted to hydrogen during off-peak hours and converted back to power using fuel cells during peak hours. Further, according to the delivered hydrogen, it is apparent that in light of the PtH technology, the procurement of hydrogen from the HPC is limited to the peak hours, when the power generated from RESs is

preferably sold to the power grid for financial gains. Figure 5 illustrates the total exchanged power of the community with the power grid and bid/offer prices. According to Fig. 5, the P&HMGs manage to sell power during high LMP period, i.e., the 17th hour to the 20th hour, while they purchase power during the rest of the day.

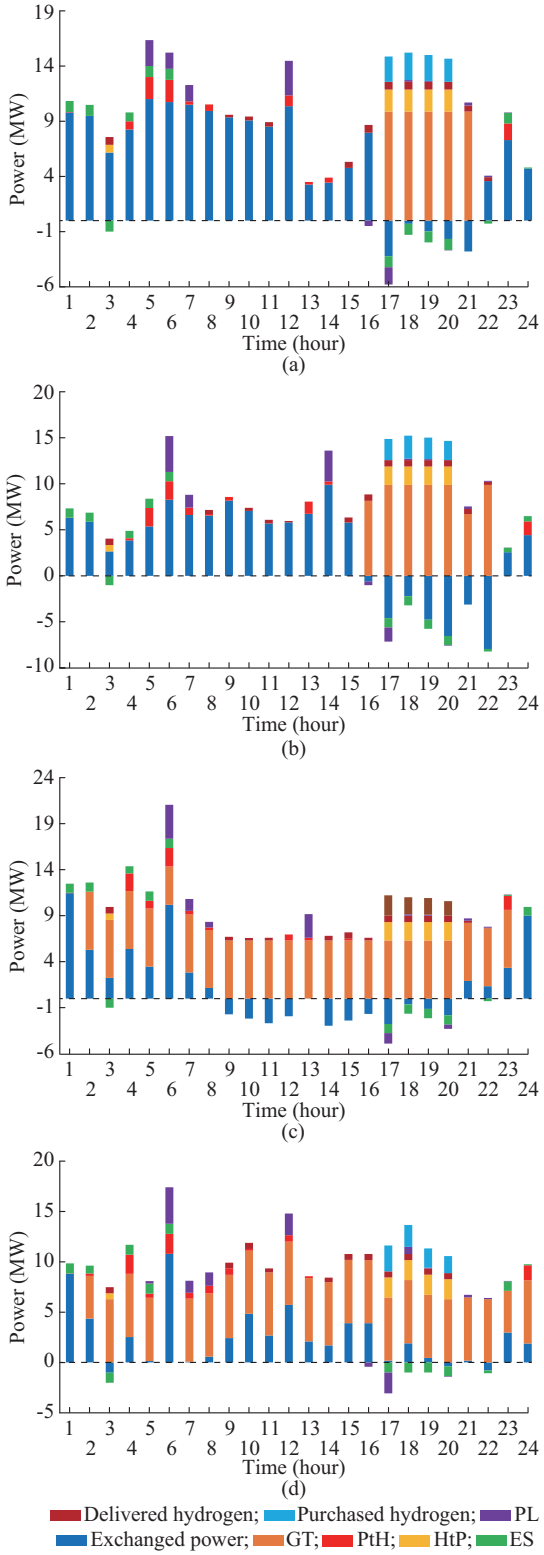

Fig. 4. Power and hydrogen dispatch of each P&HMG. (a) P&HMG 1. (b) P&HMG 2. (c) P&HMG 3. (d) P&HMG 4.

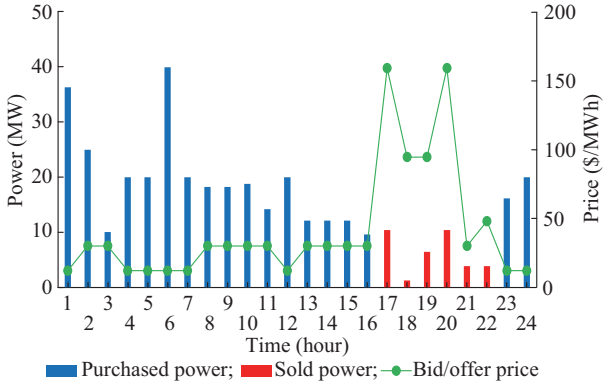

Fig. 5. Total exchanged power of community with power grid and bid/offer prices.

Table II presents the operation costs of the P&HMGs under strategic and non-strategic behaviors on modified IEEE 6-bus system. Non-strategic behavior assumes that the problem is solved from the perspective of transmission system as a single-level problem that maximizes social welfare. Overall, according to the supplied statistics, P&HMGs could achieve lower operation cost under the strategic behavior. Specifically, the total operation cost of all P&HMGs with no flexibility under the strategic behavior is $359.793 (1.94%) less than that under the non-strategic behavior. This amount increases to $719.459 (4.59%) with the inclusion of ES and V2G technologies and $946.794 (7.02%) by considering the full flexibility including ES, V2G, PtH, and HtP. Furthermore, Table II demonstrates that the P&HMGs can benefit more from their flexible technologies under the strategic behavior. For instance, the utilization of all flexible technologies under the non-strategic behavior results in a cost reduction of $5031.3 (27.19%), whereas under the strategic behavior, this value increases to $5618.3 (30.96%).

Table III compares the impact of the BiLSTM network against other deep learning methods on the operation cost of P&HMGs. The average errors of all P&HMGs under recurrent neural network (RNN), LSTM network, and BiLSTM network in relation to the real data are recorded as 5.59%, 3.48%, and 1.68%, respectively. As can be observed, the BiLSTM network outperforms the other two well-known deep learning methods. Moreover, Fig. 6 shows the impact of the RO on the operation cost of P&HMGs. To this end, the optimization problem was solved for different uncertainty budgets starting from 0 (indicating no uncertainty) to 2 (indicating full uncertainty). According to the results obtained, by increasing the value of the uncertainty budget, the operation costs increase. This phenomenon occurs because as the value of the uncertainty budget increases, the RO dispatches less RES output power. Finally, Table IV analyzes the performance of the proposed approach. Since the proposed approach is sensitive to the parameter ρ, a sensitivity analysis inspired by [34] is conducted. As shown in Table IV, the proposed approach does not converge for $\rho < N$, $\rho = N$, and $\rho = 10$ after 400 iterations. However, for $\rho = 100$, the proposed approach converges within 26 iterations. It is also observed that the proposed approach outperforms the traditional ADMM by converging 11 iterations faster. Fur-

thermore, Table V shows the impact of the stopping criteria *er* on the convergence of the proposed approach with $\rho = 100$. As can be observed, a higher *er* causes a faster convergence, but at the cost of higher residual values. However, the residual values decrease to an acceptable range by reducing *er*, at the cost of a few more iterations.

TABLE II
OPERATION COSTS OF P&HMGS UNDER STRATEGIC AND NON-STRATEGIC BEHAVIORS ON MODIFIED IEEE 6-BUS SYSTEM

P&HMG	Operation cost under non-strategic behavior ($)			Operation cost under strategic behavior ($)		
	No flexibility	ES + V2G	ES + V2G + PtH + HtP	No flexibility	ES + V2G	ES + V2G + PtH + HtP
1	6106.002	5469.827	4861.884	6039.904	5315.096	4632.358
2	3460.039	3097.766	2752.289	3391.281	2835.978	2342.972
3	3406.923	2516.228	2034.854	3317.331	2424.877	1906.039
4	5528.557	4581.977	3821.196	5393.212	4370.388	3642.060

TABLE III
IMPACT OF BILSTM NETWORK AGAINST OTHER DEEP LEARNING METHODS ON OPERATION COST OF P&HMGS

P&HMG	Operation cost ($)			
	RNN	LSTM	BiLSTM	Real data
1	4515.793	4573.578	4632.358	4693.771
2	2082.815	2158.689	2342.972	2265.589
3	1748.999	1792.177	1906.039	1883.895
4	3749.201	3631.644	3642.060	3676.501

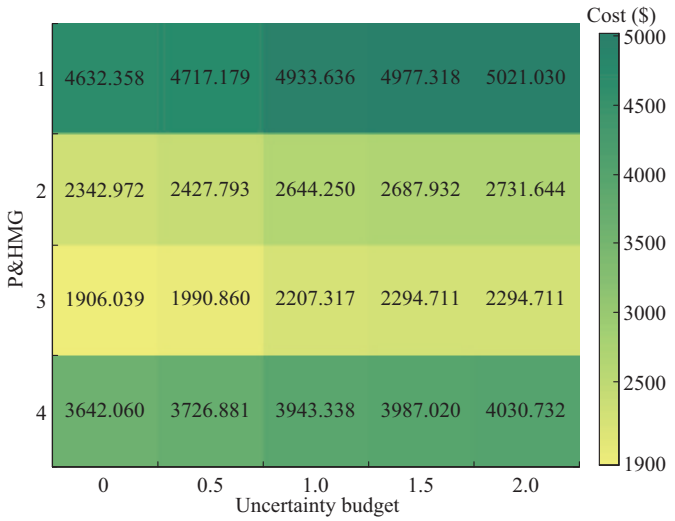

Fig. 6. Impact of RO on operation cost of P&HMGs.

TABLE IV
PERFORMANCE ANALYSIS OF PROPOSED APPROACH

ρ	Residual calculated based on (5b)	Number of iterations	
		Proposed approach	Traditional ADMM
$< N$	> 4.000	400	
N	2.790	400	
10	1.100	400	
100	< 0.001	26	37

C. Modified IEEE 24-bus System

In this case study, six P&HMGs are interconnected with bus 14 of the IEEE 24-bus system. The data related to this case study are available in [35]. In this case study, the proposed approach converges within 176 iterations with a residual value of less than 10^{-3}. The operation costs of P&HMGs under strategic and non-strategic behaviors on modified IEEE 24-bus system are shown in Table VI. According to the findings, the total operation cost of all P&HMGs with no flexibility under the strategic behavior is $151.384 (0.99%) less than that under the non-strategic behavior. With the incorporation of ES and V2G, this difference increases to $200.163 (1.32%). In addition, through optimal utilization of all flexible technologies, the difference can be increased to $484.337 (3.86%). Moreover, it is observed that the community of P&HMGs could benefit from the flexible technologies, especially hydrogen-based technologies, to reduce the total operation costs by $2683.59 (17.65%) under the non-strategic behavior and by $3016.55 (20.04%) under the strategic behavior—an improvement of 2.39 percentage points.

TABLE V
IMPACT OF STOPPING CRITERIA ON CONVERGENCE OF PROPOSED APPROACH WITH $\rho = 100$

er	Number of iterations	Residual
0.100	19	0.03510
0.010	26	0.00058
0.001	31	0

V. CONCLUSION

In this study, a decentralized energy management model was developed for P&HMGs. This model facilitates collaboration among P&HMGs to participate in the WEM while adapting a strategic behavior. To preserve the privacy of P&HMGs, and enhance the security and scalability of the model, a fast ADMM running on an MEC system was proposed as a decentralized energy management approach to solve the problem in a decentralized manner. In addition, a BiLSTM network was taken into account to deal with the uncertainty. Test results from IEEE 6-bus and 24-bus systems reveal that the proposed model reduces the total operation cost of P&HMGs by about 7.02% and 3.86%, respectively, compared with the one under non-strategic behavior. Furthermore, the proposed model successfully converged in both case studies, demonstrating its potential for large-scale implementation.

TABLE VI
OPERATION COSTS OF P&HMGS UNDER STRATEGIC AND NON-STRATEGIC BEHAVIORS ON MODIFIED IEEE 24-BUS SYSTEM

P&HMG	Operation cost ($)						
	Non-strategic behavior			Strategic behavior			Robust strategic behavior
	No flexibility	ES + V2G	ES + V2G + PtH + HtP	No flexibility	ES+V2G	ES + V2G + PtH + HtP	
1	2782.748	2769.283	2350.551	2747.361	2727.375	2203.707	2467.523
2	1886.851	1864.684	1460.806	1874.984	1855.650	1332.951	1597.448
3	1512.743	1498.347	1110.666	1503.518	1483.065	1074.710	1342.349
4	2531.634	2511.917	2012.066	2513.936	2493.824	1980.522	2244.123
5	3965.091	3944.736	3566.087	3913.365	3891.538	3483.125	3743.316
6	2523.559	2511.392	2018.856	2498.078	2478.744	1959.680	2228.723

Future research directions could explore alternative methodologies for addressing bi-level optimization problems. Additionally, enhancements to the proposed approach could be made to improve its speed of convergence. Lastly, this study could be extended by considering other types of electricity markets such as the balancing market.

REFERENCES

[1] S. Liu, L. Wang, J. Hu *et al*., "A stochastic charging station deployment model for electrified taxi fleets in coupled urban transportation and power distribution networks," *IEEE Transactions on Sustainable Energy*, vol. 15, no. 2, pp. 1138-1150, Apr. 2024.

[2] U. Tietge, P. Mock, N. Lutsey *et al*., "Comparison of leading electric vehicle policy and deployment in Europe," *International Council Clean Transportation*, vol. 49, pp. 847 129-102, May 2016.

[3] National Grid. (2023, May). Delivering for 2035: upgrading the grid for a secure, clean and affordable energy future. [Online]. Available: https://www.nationalgrid.com/document/149496/download

[4] Department for Energy Security and Net Zero. (2021, Aug.). UK hydrogen strategy. [Online]. Available: https://assets. publishing. service. gov.uk/media/64c7e8bad8b1a70011b05e38/UK-Hydrogen-Strategy_web. pdf

[5] NESO. (2025, Jan.). National grid ESO. [Online]. Available: https://www.nationalgrideso.com/

[6] M. Daneshvar, B. Mohammadi-Ivatloo, and K. Zare, "A fair risk-averse stochastic transactive energy model for 100% renewable multi-microgrids in the modern power and gas incorporated network," *IEEE Transactions on Smart Grid*, vol. 14, no. 3, pp. 1933-1945, May 2023.

[7] A. M. Saatloo, A. Mehrabi, M. Marzband *et al*., "Hierarchical user-driven trajectory planning and charging scheduling of autonomous electric vehicles," *IEEE Transactions on Transportation Electrification*, vol. 9, no. 1, pp. 1736-1749, Mar. 2023.

[8] Z. Liu, Y. Xu, C. Zhang *et al*., "A blockchain-based trustworthy collaborative power trading scheme for 5G-enabled social internet of vehicles," *Digital Communications and Networks*, vol. 8, no. 6, pp. 976-983, Dec. 2022.

[9] L. K. Gan, P. Zhang, J. Lee *et al*., "Data-driven energy management system with Gaussian process forecasting and MPC for interconnected microgrids," *IEEE Transactions on Sustainable Energy*, vol. 12, no. 1, pp. 695-704, Jan. 2021.

[10] T. Niu, H. Li, G. Chen *et al*., "Pricing and distributed scheduling framework of multi-microgrid system based on coupled electricity-carbon market," *Journal of Modern Power Systems and Clean Energy*, vol. 13, no. 3, pp. 1026-1039, May 2025.

[11] J. Zhu, D. Li, Y. Chen *et al*., "Parallel hybrid deep reinforcement learning for real-time energy management of microgrid," *Journal of Modern Power Systems and Clean Energy*, vol. 13, no. 3, pp. 991-1002, May 2025.

[12] X. Li, C. Li, G. Chen *et al*., "A risk-averse energy sharing market game for renewable energy microgrid aggregators," *IEEE Transactions on Power Systems*, vol. 37, no. 5, pp. 3528-3539, Sept. 2022.

[13] A. M. Saatloo, A. Mehrabi, M. Marzband *et al*., "Local energy market design for power- and hydrogen-based microgrids considering a hybrid uncertainty controlling approach," *IEEE Transactions on Sustainable Energy*, vol. 15, no. 1, pp. 398-413, Jan. 2024.

[14] Y. Pu, Q. Li, S. Luo *et al*., "Peer-to-peer electricity-hydrogen trading among integrated energy systems considering hydrogen delivery and transportation," *IEEE Transactions on Power Systems*, vol. 39, no. 2, pp. 3895-3911, Mar. 2024.

[15] A. Noutash and M. Kalantar, "Integration of mobile power-hydrogen storage systems in distribution-level networks: a fuzzy information gap optimization framework," *Sustainable Cities and Society*, vol. 101, p. 105166, Feb. 2024.

[16] H. Wang, X. Wang, and Z. Fu, "Energy management strategy for optimal charge depletion of plug-in FCHEV based on multi-constrained deep reinforcement learning," *IEEE Transactions on Transportation Electrification*, vol. 11, no. 1, pp. 1077-1090, Feb. 2025.

[17] Z. M. Shoja, M. A. Mirzaei, H. Seyedi *et al*., "Sustainable energy supply of electric vehicle charging parks and hydrogen refueling stations integrated in local energy systems under a risk-averse optimization strategy," *Journal of Energy Storage*, vol. 55, p. 105633, Nov. 2022.

[18] W. Kong, K. Sun, and J. Zhao, "Two-stage optimal scheduling of community integrated energy system considering operation sequences of hydrogen energy storage systems," *Journal of Modern Power Systems and Clean Energy*, vol. 13, no. 1, pp. 276-288, Jan. 2025.

[19] G. Sun, G. Li, P. Li *et al*., "Coordinated operation of hydrogen-integrated urban transportation and power distribution networks considering fuel cell electric vehicles," *IEEE Transactions on Industry Applications*, vol. 58, no. 2, pp. 2652-2665, Mar. 2022.

[20] A. Ravi, L. Bai, V. Cecchi *et al*., "Stochastic strategic participation of active distribution networks with high-penetration DERs in wholesale electricity markets," *IEEE Transactions on Smart Grid*, vol. 14, no. 2, pp. 1515-1527, Mar. 2023.

[21] M. A. Mirzaei, H. Mehrjerdi, and A. M. Saatloo, "Robust strategic behavior of a large multi-energy consumer in electricity market considering integrated demand response," *IEEE Systems Journal*, vol. 17, no. 4, pp. 6346-6356, Dec. 2023.

[22] N. Nasiri, A. Mansour Saatloo, M. A. Mirzaei *et al*., "A robust bi-level optimization framework for participation of multi-energy service providers in integrated power and natural gas markets," *Applied Energy*, vol. 340, p. 121047, Jun. 2023.

[23] J. Wang, Z. Wang, B. Yang *et al*., "V2G for frequency regulation service: a Stackelberg game approach considering endogenous uncertainties," *IEEE Transactions on Transportation Electrification*, vol. 11, no. 1, pp. 463-475, Feb. 2025.

[24] Y. Ren, M. Tan, Y. Su *et al*., "Two-stage adaptive robust charging scheduling of electric vehicle station based on hybrid demand response," *IEEE Transactions on Transportation Electrification*, vol. 11, no. 1, pp. 1442-1454, Feb. 2025.

[25] Y. Zhou, Q. Zhai, Z. Xu *et al*., "Multi-stage adaptive stochastic-robust scheduling method with affine decision policies for hydrogen-based multi-energy microgrid," *IEEE Transactions on Smart Grid*, vol. 15, no. 3, pp. 2738-2750, May 2024.

[26] Z. Liu, B. Huang, X. Hu *et al*., "Blockchain-based renewable energy trading using information entropy theory," *IEEE Transactions on Network Science and Engineering*, vol. 11, no. 6, pp. 5564-5575, Nov.-Dec. 2024.

[27] Z. Chen, Z. Li, D. Lin *et al*., "Multi-time-scale optimal scheduling of integrated energy system with electric-thermal-hydrogen hybrid energy storage under wind and solar uncertainties," *Journal of Modern Power Systems and Clean Energy*, vol. 13, no. 3, pp. 904-914, May 2025.

[28] D. Bertsimas and M. Sim, "The price of robustness," *Operations Research*, vol. 52, no. 1, pp. 35-53, Feb. 2004.

[29] J. Fortuny-Amat and B. McCarl, "A representation and economic interpretation of a two-level programming problem," *Journal of the Opera-*

tional Research Society, vol. 32, no. 9, pp. 783-792, Sept. 1981.
[30] S. Boyd, "Distributed optimization and statistical learning *via* the alternating direction method of multipliers," *Foundations and Trends in Machine Learning*, vol. 3, no. 1, pp. 1-122, Jul. 2010.
[31] T. Goldstein, B. O'Donoghue, S. Setzer *et al*., "Fast alternating direction optimization methods," *SIAM Journal on Imaging Sciences*, vol. 7, no. 3, pp. 1588-1623, Jan. 2014.
[32] M. S. Bazaraa, J. J. Jarvis, and H. D. Sherali, *Linear Programming and Network Flows*. Hoboken: John Wiley & Sons, 2011.
[33] Data Platform. (2020, Oct.). Load, wind and solar, prices in hourly resolution. [Online]. Available: https://data. open-power-system-data. org/time_series/
[34] J. L. Crespo-Vazquez, T. AlSkaif, A. M. Gonzalez-Rueda *et al*., "A community-based energy market design using decentralized decision-making under uncertainty," *IEEE Transactions on Smart Grid*, vol. 12, no. 2, pp. 1782-1793, Mar. 2021.
[35] C. Ordoudis, P. Pinson, J. M. M. Morales *et al*. (2016, Jun.). An updated version of the IEEE RTS 24-bus system for electricity market and power system operation studies. [Online]. Available: https://backend.orbit.dtu.dk/ws/portalfiles/portal/120568114/An_Updated_Version_of_the_IEEE_RTS_24Bus_System_for_Electricty_Market_an....pdf

Amin Mansour Saatloo received the B.Sc. and M.Sc. degrees in power system engineering from the Urmia University, Urmia, Iran, and the University of Tabriz, Tabriz, Iran, respectively, and the Ph.D. degree from Northumbria University, Newcastle upon Tyne, UK, in power systems engineering. Currently, he works as a Junior Power System Consultant at Rina Tech UK Ltd., Manchester, UK. His research interests mainly focus on power system connection compliance.

Abbas Mehrabi received the B. Sc. and M. Sc. degrees in computer engineering from the University of Kerman, South Tehran, Iran, and the Azad University, South Tehran, Iran, in 2008 and 2010, respectively, and the Ph. D. degree from the School of Electrical Engineering and Computer Science, Gwangju Institute of Science and Technology, Gwangju, South Korea, in 2017. He is currently an Assistant Professor with the Department of Computer and Information Sciences, Northumbria University, Newcastle upon Tyne, UK. His research interests include mobile cloud/edge computing, smart grid communication, Internet of Things, and vehicular networking.

Nauman Aslam is a Professor in the Department of Computer and Information Science, Northumbria University, Newcastle upon Tyne, UK. His current research interests include problems related to wireless body area networks and Internet of Things, network security, charging management of electric vehicles, and application of artificial intelligence in communication networks.

Mousa Marzband received the Ph. D. degree in electrical power systems from Universitat Politècnica de Catalunya (UPC), Barcelona, Spain, under a full scholarship from the Catalonia Institute for Energy Research (IREC), Barcelona, Spain. He is currently a Professor and Chair of Energy Transition at King Abdulaziz University, Jeddah, Saudi Arabia. His research interests include smart grid, renewable energy integration, energy management system, and advanced control strategy for net-zero energy systems.